LHCb pentaquarks as a baryon-$\psi(2S)$ bound state: Prediction of isospin-$\frac{3}{2}$ pentaquarks with hidden charm

Irina A. Perevalova,[1] Maxim V. Polyakov,[2,3] and Peter Schweitzer[4,5]

[1]*Physics Department, Irkutsk State University, Karl Marx str. 1, 664003 Irkutsk, Russia*
[2]*Petersburg Nuclear Physics Institute, Gatchina, 188300, St. Petersburg, Russia*
[3]*Institut für Theoretische Physik II, Ruhr-Universität Bochum, D-44780 Bochum, Germany*
[4]*Department of Physics, University of Connecticut, Storrs, Connecticut 06269, USA*
[5]*Institute for Theoretical Physics, Tübingen University, Auf der Morgenstelle 14, 72076 Tübingen, Germany*

(Received 25 August 2016; published 20 September 2016)

The pentaquark $P_c^+(4450)$ recently discovered by the LHCb has been interpreted as a bound state of $\Psi(2S)$ and a nucleon. The charmonium-nucleon interaction which provides the binding mechanism is given, in the heavy-quark limit, in terms of charmonium chromoelectric polarizabilities and densities of the nucleon energy-momentum tensor. In this work, we show in a model-independent way, by exploring general properties of the effective interaction, that $\Psi(2S)$ can form bound states with a nucleon and Δ. Using the Skyrme model to evaluate the effective interaction in the large-N_c limit and estimate $1/N_c$ corrections, we confirm the results from prior work which were based on a different effective model (chiral quark soliton model). This shows that the interpretation of $P_c^+(4450)$ is remarkably robust and weakly dependent on the details of the effective theories for the nucleon energy-momentum tensor. We explore the formalism further and present robust predictions of isospin-$\frac{3}{2}$ bound states of $\Psi(2S)$ and Δ with masses around 4.5 GeV and widths around 70 MeV. The approach also predicts broader resonances in the $\Psi(2S)$-Δ channel at 4.9 GeV with widths of the order of 150 MeV. We discuss in which reactions these new isospin-$\frac{3}{2}$ pentaquarks with hidden charm can be observed.

DOI: 10.1103/PhysRevD.94.054024

I. INTRODUCTION

The LHCb Collaboration has recently discovered new pentaquark states by studying the decays of $\Lambda_b^0 \to J/\Psi p K^-$ [1]. This decay channel is dominated by the weak decay $\Lambda_b^0 \to J/\Psi \Lambda^*$ with subsequent strong decays $\Lambda^* \to pK^-$. However, the $J/\Psi p$ spectrum contains structures which can be interpreted as exotic pentaquark "P_c^+" ($c\bar{c}uud$) resonances. In about $(8.4 \pm 0.7 \pm 4.2)\%$ of the cases, a broad resonance $P_c^+(4380)$ is formed, and in about $(4.1 \pm 0.5 \pm 1.1)\%$ of the cases, a narrow resonance $P_c^+(4450)$ is formed. Their properties are summarized in Table I. The analysis of Ref. [1] is supported by the LHCb study [2] where it was shown in a model-independent way that $K^- p$ resonant or nonresonant contributions alone cannot explain the structures seen in the $\Lambda_b^0 \to J/\Psi p K^-$ decays. The recent LHCb analysis of the $\Lambda_b^0 \to J/\psi p \pi^-$ decays provides further support for the existence of the new pentaquark states [3].

The new states have been interpreted in a variety of theoretical approaches. For instance, it was considered that they are loosely bound ("molecular") charmed baryon-meson states [4] and bound states of light and heavy diquarks including c-quarks [5], and even the possibility of open-color bound states was considered [6]. Also, the possibility was discussed that the observed structures could arise from threshold cusp effects [7].

In this work, we will use the formalism developed in Ref. [8] where the narrow $P_c^+(4450)$ state was interpreted as a nucleon-$\psi(2S)$ s-wave bound state with $J^P = \frac{3}{2}^-$. In this approach, the binding mechanism is provided by the effective charmonium-nucleon interaction, which is given by the product of the charmonium chromoelectric polarizability and the nucleon energy-momentum tensor (EMT) densities. In Ref. [8], also a $J^P = \frac{1}{2}^-$ state was predicted with nearly the same mass as $P_c^+(4450)$ (modulo hyperfine splitting due to quarkonium-nucleon spin-spin interaction which are suppressed in the heavy-quark mass limit by $1/m_Q$). The broader resonance $P_c(4380)$ does not appear as a nucleon-$\psi(2S)$ bound state in Ref. [8]. Notice that no nucleon-J/Ψ bound states exist in this formalism as the effective interaction is too weak in this channel.

The purpose of our study is to confirm the findings of Ref. [8] and to investigate whether the formalism predicts

TABLE I. Summary of properties of the new pentaquark states observed at the LHCb [1].

State	Mass (MeV)	Width (MeV)	Isospin	Spin-parity J^P
$P_c^+(4380)$	$4380 \pm 8 \pm 29$	$205 \pm 18 \pm 86$	$\frac{1}{2}$	$\frac{3}{2}^-$ or $\frac{3}{2}^+$ or $\frac{5}{2}^+$
$P_c^+(4450)$	$4449.8 \pm 1.7 \pm 2.5$	$39 \pm 5 \pm 19$	$\frac{1}{2}$	$\frac{5}{2}^+$ or $\frac{5}{2}^-$ or $\frac{3}{2}^-$

further bound states which could allow us to test this approach. For that, we will first derive a model-independent lower bound which the chromoelectric polarizability must satisfy such that charmonium-baryon bound states can exist. This derivation only makes use of general properties of the effective baryon-charmonium interaction. We will apply this bound to show in a model-independent way that $\psi(2S)$ can form s-wave bound states with a nucleon and Δ.

Specific predictions require the use of a model for the nonperturbative calculation of the EMT densities of baryons. For that, in Ref. [8], results were used from the chiral quark soliton model [9]. In this work, we will use a different model for EMT densities, namely, the Skyrme model [10]. This model is based on chiral symmetry and the $1/N_c$ expansion like the chiral quark soliton model. But it differs in many important respects and is therefore well suited to provide an important cross-check. Our results in the Skyrme model will confirm in detail the calculation of Ref. [8].

The chiral soliton model and the Skyrme model describe baryons as chiral solitons in the limit of a large number of colors N_c and provide different practical realizations of the picture of baryons in the large-N_c limit of QCD [11]. In nature, $N_c = 3$ does not seem large, and one may wonder whether $1/N_c$ corrections could affect our description of the new pentaquark states. We will therefore use the Skyrme model to investigate also the role of $1/N_c$ corrections. For that, we will establish a procedure to construct a conserved EMT when a theory cannot be solved exactly and certain (in our case $1/N_c$) corrections must be included as a small perturbation. We will show that our description of the hidden charm pentaquarks is remarkably robust, also when one includes $1/N_c$ corrections.

Our study of the $1/N_c$ corrections to the EMT has interesting byproducts. Soliton models based on the large-N_c expansion describe baryons with spin and isospin quantum numbers $S = I = \frac{1}{2}, \frac{3}{2}, \frac{5}{2}, \ldots$ as different rotational states of the same soliton solution [throughout this work, we focus on the SU(2) flavor sector]. In contrast to the quantum numbers $S = I = \frac{1}{2}$ and $\frac{3}{2}$, which correspond, respectively, to the nucleon and Δ, the quantum numbers $S = I \geq \frac{5}{2}$ are not observed. This is considered an unsatisfactory artifact of the (rigid rotator) soliton approach. Our study will shed new light on this issue. We will show that $1/N_c$ corrections constitute a "reasonably small perturbation" in the nucleon case. They are more sizable for Δ, but we find that also in this case it is possible to reconstruct a conserved EMT which satisfies basic criteria for mechanical stability. However, we will show that for $S = I \geq \frac{5}{2}$ this is not possible; here, $1/N_c$ corrections are simply too destabilizing. In this way, the rotating soliton approach provides an explanation why the quantum numbers $S = I \geq \frac{5}{2}$ are not realized in nature. As another byproduct, we will discuss the EMT of the Δ and show that it has a negative D term in agreement with theoretical studies of other particles.

The main application in this context is, however, to investigate the question of whether charmonia can bind with the Δ resonance. We will show that J/Ψ does not form bound states with Δ. But in the Δ-$\psi(2S)$ channel, the formalism makes robust predictions of bound states and also predicts resonant states, albeit with somewhat larger theoretical uncertainties. We will make specific predictions for the masses, widths, spins, and parities of the new states. Finally, we will discuss in which reactions the new states could in principle be observed.

II. EFFECTIVE QUARKONIUM-BARYON INTERACTION

In this section, we review the derivation of the effective quarkonium-baryon potential and describe how it can be expressed in terms of EMT densities.

A. Effective potential

The description of hidden-charmonium pentaquark states of Ref. [8] explores the fact that heavy charmonium states are small compared to the nucleon size, and their interaction with baryons is relatively weak on the typical scale for strong interactions. In this situation, a nonrelativistic multipole expansion can be applied [12].

The multipole expansion reveals that the dominant mechanism for the baryon-quarkonium interaction is the emission of two virtual chromoelectric dipole gluons in a color singlet state. The potential describing the effective interaction is proportional to the product of the quarkonium chromoelectric polarizability and the gluon energy-momentum density in the nucleon [13]. The small parameter justifying this derivation is given by the ratio of the quarkonium size to the effective gluon wavelength. The resulting effective dipole Lagrangian is given by [14]

$$L_{\rm eff} = -V_{\rm eff}, \qquad V_{\rm eff} = -\frac{1}{2}\alpha \boldsymbol{E}^2, \tag{1}$$

where α denotes the chromoelectric polarizability in the channel of interest and $\boldsymbol{E}$ is the chromoelectric gluon field, the definition of which includes the strong coupling constant g renormalized at the quarkonium mass scale.

B. Chromoelectric polarizabilities

The chromoelectric polarizabilities can be calculated in the heavy-quark approximation and large-N_c limit, where the quarkonia are described as Coulomb systems in lowest-order approximation, with the results given by [8,15]

$$\alpha(1S) \approx 0.2\ \text{GeV}^{-3}(\text{pert}), \tag{2a}$$

$$\alpha(2S) \approx 12\ \text{GeV}^{-3}(\text{pert}), \tag{2b}$$

$$\alpha(2S \to 1S) \approx \begin{cases} -0.6\ \text{GeV}^{-3}(\text{pert}), \\ \pm 2\ \text{GeV}^{-3}(\text{pheno}). \end{cases} \tag{2c}$$

In Eq. (2c), we included also the phenomenological value for the polarizability of the $2S \to 1S$ transition inferred from analyses of $\psi' \to J/\psi\pi\pi$ data [13] (such studies only allow extracting the modulus of the transitional polarizability). For $\alpha(1S)$, the $1/N_c$ corrections are merely of order of 5% [16]. But for $\alpha(2S)$ and higher polarizabilities, the effects of $1/N_c$ corrections are not known, and the comparison of the perturbative and phenomenological results in Eq. (2c) indicates that at present the chromoelectric polarizabilities are not well understood. Below, we will therefore use the values quoted in Eq. (2) not at their bare values but as guidelines.

For $\psi(nS)$ with $n \geq 3$, the perturbative results for polarizabilities grow rapidly with n as $\alpha(nS) \propto n^2(7n^2-3)$ [15] because the size of the system grows. In this situation, the Coulomb approximation becomes worse, and the usefulness of perturbative predictions for $\psi(3S)$ and higher states becomes questionable.

C. Relation to EMT densities

The effective interaction in Eq. (1) can be expressed in terms of the densities of the nucleon EMT. This can be done exploring the conformal anomaly [17] to relate $\boldsymbol{E}^2$ in Eq. (1) to the trace $T^{\mu}{}_{\mu}$ of the EMT of QCD and the gluon contribution to the energy density T^G_{00}. The latter can be related as $T^G_{00} = \xi_s T_{00}$ to the total energy density T_{00} of the nucleon where the parameter ξ_s describes the fraction of the nucleon energy due to gluons at the scale μ_s [18]. Neglecting a numerically small term due to the current masses of light quarks, one obtains [8]

$$\boldsymbol{E}^2 = g^2\left(\frac{8\pi^2}{bg_s^2}T^{\mu}{}_{\mu} + \xi_s T_{00}\right) = \frac{8\pi^2}{b}\frac{g^2}{g_s^2}(\nu T_{00} + T^k{}_k),$$
$$\nu = 1 + \xi_s\frac{bg_s^2}{8\pi^2}, \tag{3}$$

where $b = (\frac{11}{3} - \frac{2}{3}N_f)$ is the leading coefficient of the Gell-Mann-Low function and g_s is the strong coupling constant renormalized at the scale μ_s. Notice that the relevant scale for nonperturbative calculations of the nucleon structure μ_s is different from the quarkonium scale at which the strong coupling g is renormalized. Recall that g enters Eq. (3) through the definition of the chromoelectric gluon field $\boldsymbol{E}$. Therefore, in general, $g_s \neq g$, although for the charmonium-nucleon potential, these two scales are comparable.

The coefficient ν introduced in Eq. (3) was estimated on the basis of the instanton liquid model of the QCD vacuum and the chiral quark soliton model, where the strong coupling constant freezes at a scale set by the nucleon size at $\alpha_s = g_s^2/(4\pi) \approx 0.5$. Assuming $\xi_s \approx 0.5$ as suggested by the fraction of nucleon momentum carried by gluons in deep-inelastic scattering at scales comparable to μ_s, one obtains the value [8]

$$\nu \approx 1.5. \tag{4}$$

A similar result $\nu = (1.45\text{–}1.6)$ was obtained for the pion in Ref. [18]. These results are supported by the analysis of the nucleon mass decomposition in Ref. [19] where $\xi_s \approx \frac{1}{3}$, leading to $\nu \approx 1.4$, which is within the accuracy of Eq. (4). We will use the value (4) for the calculations in this work.

III. SUFFICIENT CONDITION FOR EXISTENCE OF A QUARKONIUM-BARYON BOUND STATE

In this section, we discuss, in a model-independent way, the lower bound for the chromoelectric polarizability at which a quarkonium-baryon bound state is formed. In Ref. [20], the sufficient condition for the existence of an s-wave bound state in a given attractive potential,

$$-\frac{2\mu}{R}\int_0^R \mathrm{d}r r^2 V(r) - 2\mu R\int_R^\infty \mathrm{d}r V(r) > 1, \tag{5}$$

was derived, where R is an arbitrary distance, μ is the reduced baryon-charmonium mass, and the attractive potential $V(r)$ is negative. We will refer to this condition as the Calogero bound in the following.

Let us consider first the nucleon case. The effective $\psi(2S)$-nucleon potential is normalized as [8]

$$\int_0^\infty \mathrm{d}r r^2 V_{\mathrm{eff}}(r) = -\alpha\frac{\pi}{b}\frac{g^2}{g_s^2}\nu M_N, \tag{6}$$

and also its large r asymptotics (in the chiral limit in leading order of the large-N_c expansion) is known [8] [see also Eq. (25) below]:

$$V_{\mathrm{eff}}(r) \sim -\alpha\frac{27}{4b}\frac{g^2}{g_s^2}(1+\nu)\frac{g_A^2}{F_\pi^2 r^6}. \tag{7}$$

Now, we can choose the parameter R in Eq. (5) large enough such that for $r > R$ the asymptotics (7) can be used. This allows us to rewrite Eq. (5) as an inequality for the chromoelectric polarizability:

$$\alpha > \frac{b}{2\pi}\frac{g_s^2}{g^2}\frac{1}{\nu}\frac{R}{\mu M_N}\left[1 - \frac{9}{10\pi}\frac{1+\nu}{\nu}\frac{g_A^2}{F_\pi^2 M_N}\frac{1}{R^3}\right]^{-1}. \tag{8}$$

Note that this inequality is model independent as it is based only on general (model-independent) properties of the effective potential (6) and (7). If we choose $R = 1.5$ fm [for that value, we are sure that asymptotic formula (7) works perfectly] and take the noncommutativity of the chiral limit and the large-N_c limit (see Appendix) into consideration, we obtain that for $\alpha > 10.7\ \mathrm{GeV}^{-3}$ the nucleon and $\psi(2S)$ must form a bound state. This value for the lower bound does not depend on details of the potential shape.

The inequality (8) can be easily generalized to any other baryon. What one needs for that is to derive the large-distance behavior of $V_{\rm eff}(r)$ for a given baryon.[1] This can be done with help of chiral perturbation theory.

For example, if one applies the Calogero lower bound to the case of the Δ resonance, one obtains that for $\alpha > 6.6\ \mathrm{GeV}^{-3}$ a charmonium-Δ bound state must form; i.e., the formation of such a bound state with isospin $3/2$ is more favorable than for the nucleon.

IV. ENERGY-MOMENTUM TENSOR AND EMT DENSITIES

In this section, we briefly introduce the form factors of the EMT, define the static EMT and the EMT densities, and review their properties which are relevant for our study.

A. Form factors and EMT densities

The nucleon form factors of the total EMT operator $\hat{T}_{\mu\nu}(0)$ are defined as [21]

$$\langle p',s'|\hat{T}_{\mu\nu}(0)|p,s\rangle = \bar{u}(p',s')\left[M_2(t)\frac{P_\mu P_\nu}{M_N} + J(t)\frac{i(P_\mu\sigma_{\nu\rho}+P_\nu\sigma_{\mu\rho})\Delta^\rho}{2M_N} + d_1(t)\frac{\Delta_\mu\Delta_\nu - g_{\mu\nu}\Delta^2}{5M_N}\right]u(p,s), \quad (9)$$

where $P=\frac{1}{2}(p'+p)$, $\Delta=(p'-p)$, $t=\Delta^2$ with nucleon states normalized as $\langle p',s'|p,s\rangle = 2p^0(2\pi)^3\delta^{(3)}(\boldsymbol{p}'-\boldsymbol{p})\delta_{s's}$. The polarizations s and s' are defined such that both correspond to the same polarization vector $\boldsymbol{s}$ in the rest frame of the corresponding nucleon. The spinors are normalized as $\bar{u}(p,s)u(p,s)=2M_N$.

In QCD, the quark and gluon contributions to the EMT are separately gauge-invariant operators and connected to observables, although only their sum is scale independent and conserved. They can be deduced from Mellin moments of the generalized parton distribution functions of quarks and gluons accessible in hard exclusive reactions.

In analogy to the electromagnetic form factors, one may introduce the static EMT in the Breit frame characterized by $\Delta^0=0$ which implies $t=-\boldsymbol{\Delta}^2$. In this frame, the static EMT is defined[2] as [22]

$$T_{\mu\nu}(\boldsymbol{r},\boldsymbol{s}) = \int\frac{d^3\boldsymbol{\Delta}}{2E(2\pi)^3}e^{i\boldsymbol{\Delta r}}\langle p',s'|\hat{T}_{\mu\nu}(0)|p,s\rangle, \quad (10)$$

where $E=E'=\sqrt{M_N^2+\frac{1}{4}\boldsymbol{\Delta}^2}$. Working with three-dimensional densities, which strictly speaking are well defined only for nonrelativistic systems, is fully consistent in our context because we will use models for the EMT based on the large-N_c limit, where baryons are heavy. This is also fully consistent with the nonrelativistic interaction (1) of heavy quarkonia with baryons and the guidelines (2) for polarizabilities calculated for heavy quarkonia in the large-N_c limit.

Let us review here the densities relevant for this work, namely, the energy density $T_{00}(\boldsymbol{r})$ and the stress tensor $T^{ij}(\boldsymbol{r})$. For a more detailed discussion of the static EMT, we refer to Ref. [22]. The energy density is normalized as

$$\int d^3\boldsymbol{r}\,T_{00}(\boldsymbol{r}) = M_N. \quad (11)$$

For a spin-$\frac{1}{2}$ particle (as well as for a spin-zero particle), the stress tensor has the general decomposition

$$T^{ij}(\boldsymbol{r}) = \left(e_r^i e_r^j - \frac{1}{3}\delta^{ij}\right)s(r) + \delta^{ij}p(r), \quad (12)$$

where $p(r)$ is the pressure and $s(r)$ is the distribution of shear forces, while $e_r^i = r^i/r$ denotes the radial unit vector and $r=|\boldsymbol{r}|$.

B. Consequences from EMT conservation

Because of EMT conservation, $s(r)$ and $p(r)$ are related to each other through the differential equation

$$\frac{2}{r}s(r)+\frac{2}{3}s'(r)+p'(r)=0, \quad (13)$$

and $p(r)$ obeys [9] the von Laue condition [23], a necessary (though not sufficient) condition for stability,

$$\int_0^\infty dr r^2 p(r) = 0. \quad (14)$$

To comply with Eq. (14), the pressure must have at least one node. Stability considerations imply that $p(r)>0$ in the inner region, which corresponds to repulsion, and $p(r)<0$ in the outer region, which corresponds to attraction, with the repulsive and attractive forces balancing exactly according to Eq. (14) [9]. An interesting quantity related to the stress tensor is the D term, which is a fundamental but unknown property [24] and expressed in terms of the pressure *or* shear forces as [22]

[1]For a baryon of mass M_B, the normalization condition is trivial,

$$\int_0^\infty dr r^2 V_{\rm eff}(r) = -\alpha\frac{\pi}{b}\frac{g^2}{g_s^2}\nu M_B.$$

[2]Notice the misprint in Eq. (5) of Ref. [22] where the factor $1/(2E)$ should appear under the integral, as written in Eq. (10).

$$d_1 = 5\pi M_N \int_0^\infty \mathrm{d}r r^4 p(r) \tag{15}$$

$$= -\frac{4\pi}{3} M_N \int_0^\infty \mathrm{d}r r^4 s(r). \tag{16}$$

In all theoretical approaches so far, the D terms of various particles were found negative.

In all expressions presented so far, $s(r)$ and $p(r)$ appear on equal footing. As long as one deals with the total EMT in a consistently solved theory, both quantities are indeed related to each other and completely equivalent. However, in some situations, one may deal with an incomplete system. One example is when one considers form factors of the quark part of the EMT in QCD. Another situation may arise when one is not able to find the exact solution but has to content oneself with an approximate solution in a(n) (effective) theory. (We will encounter exactly this situation below.)

In such situations, working with $s(r)$ is preferable over $p(r)$ for the following reason. If one deals with only a part of the system, e.g., with the quark contribution to the EMT, then there is a fourth form factor in Eq. (9) which is proportional to the structure $g^{\mu\nu}$ (the gluon part of the EMT has the same form factor but with opposite sign, such that in the total quark + gluon EMT these terms drop out). Now, we have seen that the pressure is associated with the trace of the stress tensor and is sensitive to terms arising from nonconservation of the EMT. In contrast to this, $s(r)$ is associated with the traceless part of the stress tensor and is therefore insensitive to EMT-nonconserving terms. Below, we will use this property to *reconstruct* from approximate results for $s(r)$ a conserved EMT.

C. Local criteria for stability

When constructing effective theories or models, it is essential to demonstrate their theoretical consistency. Hereby, the perhaps most important point concerns the stability of the studied solution. The von Laue condition (14) provides a useful global criterion, which was shown to be satisfied in various approaches including nuclei, nucleons, pions, Skyrmions, and Q-balls where the solutions were absolutely stable [9,10,25–29]. But also metastable and unstable solutions satisfy the von Laue condition [29–31], which means it is a necessary but not sufficient condition for stability.

For our purposes, it will be convenient to establish a necessary local stability condition. Local in our context means that it is not integrated over r like the von Laue condition. For that, we explore the analogy to classical continuum theory. This is well justified in our context, since we have in mind to apply the criteria to a semiclassical description of the nucleon in terms of a large-N_c mean field solution. An intuitive criterion is the positivity of the energy density

$$T_{00}(r) \geq 0. \tag{17}$$

In classical continuum mechanics, it follows from considering that every (also infinitesimally small) piece of volume makes a positive contribution to the energy of the system.

A less trivial local criterion can be obtained by considering that at any chosen distance r the force exhibited by the system on an infinitesimal piece of area $\mathrm{d}A e_r^i$ must be directed outward. If this was not the case, the system would collapse. Since this force is $F^i(\boldsymbol{r}) = T^{ij}(\boldsymbol{r})\mathrm{d}A e_r^j = [\frac{2}{3}s(r) + p(r)]\mathrm{d}A e_r^i$, we obtain the criterion

$$\frac{2}{3}s(r) + p(r) > 0. \tag{18}$$

We checked that the condition (18) is satisfied in all systems we are aware of where EMT densities were studied [9,10,25–31]. As this includes unstable systems, apparently also Eq. (18) is a necessary but not sufficient condition for stability. Because of its local character, it provides a stronger criterion than the von Laue condition (14) and will play an important role below. Interestingly, the criterion (18) allows one to draw a conclusion on the sign of the D term. We see that

$$0 < 4\pi \int_0^\infty \mathrm{d}r r^4 \left(\frac{2}{3}s(r) + p(r)\right)$$
$$= -\frac{2d_1}{M_N} + \frac{4d_1}{5M_N} = -\frac{6d_1}{5M_N}. \tag{19}$$

Thus, if a system satisfies the local stability criterion (18), then it must necessarily have a negative D term [but a negative D term does not imply that $s(r)$ and $p(r)$ satisfy Eq. (18), so the opposite is in general not true]. Indeed, in all systems studied so far, the D terms were found to be negative [9,10,25–31].

It would be natural to expect that the criteria (17), (18) hold also in quantum field theory, although in this case more care is needed. Investigations in this direction are left to future studies.

D. Chiral properties of densities

The leading large-distance dependence of the densities is determined by chiral physics and can be derived in any (effective) theory which consistently describes chiral symmetry breaking. Soliton models are particularly convenient for that [9,10]. In the chiral limit in leading order of the large-N_c expansion, the densities behave as, see Appendix,

$$T_{00}(r) = 3F_\pi^2 R_0^4 \frac{1}{r^6} + \ldots, \tag{20a}$$

$$p(r) = -F_\pi^2 R_0^4 \frac{1}{r^6} + \ldots, \tag{20b}$$

$$s(r) = 3F_\pi^2 R_0^4 \frac{1}{r^6} + \ldots, \tag{20c}$$

where the dots indicate terms vanishing faster than the displayed leading terms. The parameter R_0 has the meaning of the soliton size in chiral soliton models and is related to the axial coupling constant $g_A = 1.26$ and the pion decay constant $F_\pi = 186$ MeV as

$$g_A = \frac{4\pi}{3} F_\pi^2 R_0^2. \tag{21}$$

In practice, one has to determine R_0 from the self-consistent profile, which minimizes the soliton energy (we will discuss this in more detail in Sec. V A), and Eq. (21) can be used to deduce the model prediction for g_A. For finite m_π, the densities exhibit exponentially suppressed Yukawa tails; see Appendix.

E. $V_{\rm eff}$ and its properties

We are now in the position to express the effective potential $V_{\rm eff}$ in Eq. (1) in terms of the EMT densities. With the trace of the stress tensor given by $T^k{}_k = -3p(r)$, the effective potential is

$$V_{\rm eff}(\boldsymbol{r}) = -\alpha \frac{4\pi^2}{b} \frac{g^2}{g_s^2} (\nu T_{00}(r) - 3p(r)). \tag{22}$$

Because of Eqs. (11) and (14), the effective potential is "normalized" as

$$\int \mathrm{d}^3 r V_{\rm eff}(\boldsymbol{r}) = -\alpha \frac{4\pi^2}{b} \frac{g^2}{g_s^2} \nu M_N. \tag{23}$$

An instructive property of the effective potential, which may provide a useful estimate for the "range" of the effective interaction, is the mean square radius

$$\langle r_{\rm eff}^2 \rangle \equiv \frac{\int \mathrm{d}^3 r r^2 V_{\rm eff}(\boldsymbol{r})}{\int \mathrm{d}^3 r V_{\rm eff}(\boldsymbol{r})} = \langle r_E^2 \rangle - \frac{12 d_1}{5\nu M_N^2}, \tag{24}$$

where $\langle r_E^2 \rangle = \int \mathrm{d}^3 r r^2 T_{00}(r) / \int \mathrm{d}^3 r T_{00}(r)$ denotes the mean square radius of the energy density. With $d_1 < 0$ found so far in all theoretical studies, one may expect $\langle r_{\rm eff}^2 \rangle > \langle r_E^2 \rangle$.

From Eqs. (20a) and (20b), we see that in the chiral limit the effective potential behaves as

$$V_{\rm eff}(\boldsymbol{r}) = -\alpha \frac{12\pi^2}{b} \frac{g^2}{g_s^2} (1+\nu) F_\pi^2 R_0^4 \frac{1}{r^6} + \ldots. \tag{25}$$

Using Eq. (21), one obtains Eq. (7) quoted in Sec. III.

V. EMT OF NUCLEON AND Δ IN SKYRME MODEL

To solidify the predictions from Ref. [8] and gain new insights on the baryon-charmonium interaction, we will use the Skyrme model [32], which respects chiral symmetry and provides a practical realization of the large-N_c picture of baryons described as solitons of mesonic fields [11]. Despite its long history dating back to Refs. [33–39], this model still provides good services and was applied to studies of the EMT in Ref. [10], which we shall explore in this work.

A. Description of baryons in Skyrme model

In this section, we briefly review the description of baryons in the Skyrme model. For a detailed account, we refer to Refs. [33,34]. The Skyrme model is based on the following effective chiral Lagrangian:

$$\begin{aligned}\mathcal{L} = {} & \frac{F_\pi^2}{16} \mathrm{tr}_{\rm F}(\partial_\mu U)(\partial^\mu U^\dagger) \\ & + \frac{1}{32e^2} \mathrm{tr}_{\rm F}[U^\dagger(\partial_\mu U), U^\dagger(\partial_\nu U)][U^\dagger(\partial^\mu U), U^\dagger(\partial^\nu U)] \\ & + \frac{m_\pi^2 F_\pi^2}{8} \mathrm{tr}_{\rm F}(U-2).\end{aligned} \tag{26}$$

Here, F_π is the pion decay constant of which the experimental value is $F_\pi = 186$ MeV, e is the dimensionless Skyrme parameter, m_π is the pion mass, and $\mathrm{tr}_{\rm F}$ denotes the trace over SU(2) matrices. In the large-N_c limit, the model parameters scale as $F_\pi = \mathcal{O}(N_c^{1/2})$, $m_\pi = \mathcal{O}(N_c^0)$, $e = \mathcal{O}(N_c^{-1/2})$ which implies $\mathcal{L} = \mathcal{O}(N_c)$. In the large-$N_c$ limit, the chiral SU(2) field U is static and assumed to have the "hedgehog" structure $U = \exp[i\boldsymbol{\tau e_r} P(r)]$ with $r = |\boldsymbol{r}|$ and $\boldsymbol{e_r} = \boldsymbol{r}/r$. The soliton profile $P(r)$ satisfies $P(0) = \pi$ which ensures that the field U has unit winding number associated with the baryon number. The large-distance behavior of $P(r)$ is dictated by chiral symmetry and is model independent; see Appendix.

In leading order of the large-N_c limit, the soliton mass is given by $M_{\rm sol} = -\int \mathrm{d}^3 r \mathcal{L} \equiv \int \mathrm{d}^3 r T_{00}(r)$, and the variation of the soliton mass, $\delta M_{\rm sol} = 0$, is exactly equivalent to the von Laue condition (14). This was proven analytically and confirmed numerically in Ref. [10], where the expressions for $T_{00}(r)$, $p(r)$ and other EMT densities were derived and evaluated in leading (LO) and next-to-leading order (NLO) of the large-N_c expansion.

The minimization of the soliton mass $\delta M_{\rm sol} = 0$ yields the soliton solution which is then projected on spin and isospin quantum numbers by considering slow rotations $U(\boldsymbol{r}) \to A(t) U(\boldsymbol{r}) A^{-1}(t)$ in Eq. (26) with $A = a_0 + i\boldsymbol{a\tau}$ and introducing conjugate momenta $\pi_b = \partial L / \partial \dot{a}_b$. One then quantizes the collective coordinates according to

$\pi_b \to -i\partial/\partial a_b$ subject to the constraint $a_0^2 + \boldsymbol{a}^2 = 1$. This yields the Hamiltonian for soliton rotations

$$H_{\rm rot} = M_{\rm sol} + \frac{\boldsymbol{J}^2}{2\Theta} = M_{\rm sol} + \frac{\boldsymbol{I}^2}{2\Theta}, \tag{27}$$

where $\boldsymbol{J}^2$ and $\boldsymbol{I}^2$ are the squared spin and isospin operators and Θ denotes the soliton moment of inertia which is a functional of the soliton profile. The Hamiltonian (27) describes states with the spin S and isospin I quantum numbers $S = I = \frac{1}{2}, \frac{3}{2}, \ldots$ with the highest possible spin equal to $N_c/2$ for general N_c. Clearly, isospin quantum numbers $I > \frac{3}{2}$ are exotic and correspond to hypothetical multiplets that are not observed in nature. We shall come back to this point below.

The above described procedure corresponds to the "projection after variation" technique used in most practical applications. Indeed, Eq. (27) implies that the mass of a baryon with quantum numbers $S = I = \frac{1}{2}, \frac{3}{2}, \ldots$ is given by

$$M_{\rm rot} = M_{\rm sol} + \frac{S(S+1)}{2\Theta} \tag{28}$$

with the "correction" due to soliton rotations assumed to be a small perturbation. Parametrically, this is the case, since the moment of inertia is $\Theta = \mathcal{O}(N_c)$ and we work in the large-N_c limit. But in practice, it is $N_c = 3$, and the "perturbation" is not necessarily small in all cases. A particularly sensitive quantity in this respect is the pressure. Including systematically $1/N_c$ corrections to the EMT modifies not only $T_{00}(r)$ leading to Eq. (28) but also $p(r)$ and $s(r)$. The pressure with included $1/N_c$ corrections satisfies the von Laue condition (14) only if one minimizes the full expression in Eq. (28). However, in the projection-after-variation technique, one only minimizes $M_{\rm sol}$, and "rotational corrections" strictly speaking spoil stability [10].

In principle, one could use the "variation after projection" technique to remedy this problem. Here, one minimizes the mass of the rotating baryon in Eq. (28), i.e., performs first the projection on the quantum numbers of the considered baryon before minimizing its mass. In this way, one ensures compliance with the von Laue condition (14). However, this procedure has a serious drawback: it is at variance with chiral symmetry as can be seen from the large-r behavior of the profile [37,38],

$$F(r) = \frac{\rm const}{r}\exp(-m_S r) \quad \text{with}$$
$$m_S^2 = m_\pi^2 - \frac{2S(S+1)}{3\Theta[P(r)]^2}. \tag{29}$$

Since $\Theta = \mathcal{O}(N_c)$, we see that for $N_c \to \infty$ we have $m_S \to m_\pi$ and recover from Eq. (29) the correct chiral behavior of the profile; see Appendix. But for finite N_c, the result is incorrect, and for small m_π, solutions do not even exist.

Chiral symmetry and stability are crucial principles. If one wants to preserve both, then none of the two methods, projection after variation nor variation after projection, is acceptable. In our context, however, we are mainly interested in gaining trustworthy insight on effects of $1/N_c$ corrections on the effective baryon-quarkonium interaction. For that reason, we will content ourselves with a pragmatic approximate solution, which (a) preserves chiral symmetry, (b) complies with the von Laue condition, and (c) gives us reliable insight about the role of $1/N_c$ corrections.

The approximate solution, which fulfills the above criteria, is as follows. In the first step, we employ the projection after variation procedure which respects chiral symmetry. This means we first minimize the soliton energy, which guarantees the correct chiral behavior of the theory and yields a *universal profile for all (light) baryons*. After this, we project the soliton solution on $S = I = \frac{1}{2}, \frac{3}{2}\ldots$ states (nucleon, Δ resonance, … where the dots indicate exotic quantum numbers not observed in nature). This yields, in the leading order of the large-N_c limit, the same EMT for all (light) baryons.

In the second step, we then add on top of the leading-order results the rotational corrections as a *small perturbation*. We do so for the energy density $T_{00}(r)$ and shear forces $s(r)$, but not for the pressure because the resulting $p(r)$ would violate the von Laue condition (14). Instead, we determine the pressure from the differential equation (13), which then automatically satisfies the von Laue condition (14). Using Eq. (13), the pressure can be expressed in terms of $s(r)$ as [notice that Eq. (13) determines $p(r)$ up to an integration constant, which we fix such that $p(r) \to 0$ for $r \to \infty$]

$$p(r)|_{\rm NLO,reconstruct} = \left(-\frac{2}{3}s(r) + 2\int_r^\infty \frac{{\rm d}\tilde{r}}{\tilde{r}}s(\tilde{r})\right)_{\rm NLO,approx}. \tag{30}$$

This procedure corresponds to the construction of a conserved EMT from approximate results for $s(r)$. It is important to notice that the starting point for this construction is $s(r)$, which is related to the traceless part of the stress tensor and therefore in general insensitive to EMT-nonconserving terms; see Sec. IV B. Below, we will show that this procedure gives a consistent estimate of $1/N_c$ corrections to EMT densities.

B. EMT densities with $1/N_c$ corrections

The expressions for the EMT densities in LO and NLO of the $1/N_c$ expansion were derived in Ref. [10]. We refer

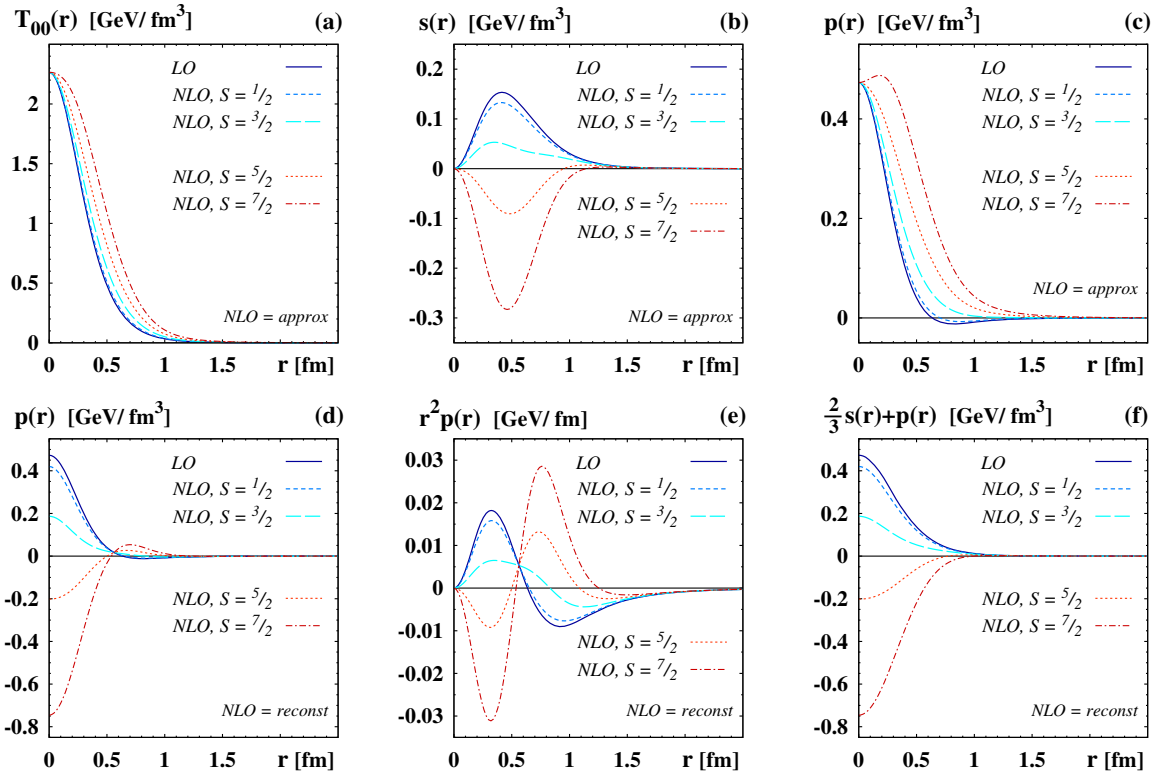

FIG. 1. EMT densities from the Skyrme model as functions of r. The LO results are valid for any $S = I$ in the large-N_c limit. The estimates of NLO corrections in the $1/N_c$ expansion are shown for states with the quantum numbers $S = I = \frac{1}{2}, \frac{3}{2}, \frac{5}{2}, \frac{7}{2}$. The figures show (a) energy density $T_{00}(r)$, (b) shear forces $s(r)$, (c) pressure $p(r)$ with approximate NLO corrections, (d) $p(r)$ with NLO corrections reconstructed according to (30), (e) same as Fig. 1(d) but for $r^2 p(r)$, and (f) the local stability criterion (18). The NLO results in the upper panel, Figs. 1(a)–1(c), are estimated by simply evaluating the NLO expressions with the LO soliton profile, which yields unacceptable results especially for $p(r)$ which are at variance with Eq. (14). The results in the lower panel, Figs. 1(d)–1(f), are obtained with the pressure reconstructed according to Eq. (30) which satisfies Eq. (14). Finally, Fig. 1(f) shows that the results for $S = I = \frac{1}{2}, \frac{3}{2}$, which correspond to the nucleon and Δ, comply with the local stability criterion (18). In contrast to this, states with the exotic quantum numbers $S = I \geq 5/2$ do not satisfy (18); i.e., in this way, the rotating soliton approach explains why they are not realized in nature.

to this work for technical details and use the same parameters[3] as Ref. [10].

Let us begin the discussion with the energy density $T_{00}(r)$. In Fig. 1(a), we show the LO result for $T_{00}(r)$ which is "universal" in the following sense. In LO of the $1/N_c$ expansion, the nucleon and Δ are mass degenerate, see Eq. (A4); i.e., both baryons have the same energy density. More precisely, $T_{00}(r)$ is the same for the entire tower of light ground-state baryons $S = I = \frac{1}{2}, \frac{3}{2}, \frac{5}{2}, \ldots$ including exotic quantum numbers. When NLO corrections due to soliton rotation are included, the mass depends on the $S = I$ quantum numbers according to Eq. (28). In Fig. 1(a), we show the associated NLO results for $T_{00}(r)$ for the states $S = \frac{1}{2}, \frac{3}{2}, \frac{5}{2}, \frac{7}{2}$ which are normalized such that $\int d^3 r T_{00}(r)$ yields the result in Eq. (28) for the mass of the respective state. From Eq. (28), it is clear that higher-spin states are heavier, and Fig. 1(a) shows that this is not due to higher density but because the "size" of the system increases with S. This makes perfectly sense in a "rigid-rotator" approach, as the NLO correction to $T_{00}(r)$ is proportional to the spin density $\rho_J(r)$ which has the behavior $\rho_J(r) \propto r^2$ in soliton models [9,10].[4] Remarkably, for $S = \frac{1}{2}$, the LO and NLO results can hardly be distinguished on the scale of Fig. 1(a). This implies that

[3]The parameters are fixed as $F_\pi = 131.3$ MeV, $e = 4.628$ with $m_\pi = 138$ MeV. This parameter choice has been optimized [10] to ensure that the respective leading results in the large-N_c expansion for the sum and difference of nucleon and Δ masses, namely, $M_\Delta + M_N \equiv 2M_{\rm sol}$ and $M_\Delta - M_N \equiv \frac{3}{2\Theta}$, reproduce the experimental values. Notice that with this fixing the experimental value of $F_\pi = 186$ MeV is underestimated by 30%, while the model results for the individual nucleon and Δ masses overestimate the physical values by about 20% [10]. This is a typical accuracy for this model [33,34]. The 20% overestimate of the baryon masses would affect the normalization of the effective potential $V_{\rm eff}$ in Eq. (23), which we shall address below in Eq. (32).

[4]The spin density $\rho_J(r)$ is associated with the form factor $J(t)$ in Eq. (9) and related to $T^{0k}(\boldsymbol{r}, \boldsymbol{s})$ components of the static EMT [22].

for the nucleon the NLO corrections are moderate. For higher spins $S=\frac{3}{2},\frac{5}{2},\frac{7}{2}$, the NLO corrections quickly become more sizable. Nevertheless, $T_{00}(r)$ does not reveal anything unusual and looks equally plausible for all spin states. Other EMT densities, namely, $s(r)$ and $p(r)$, will turn out more insightful and give us a hint why the quantum numbers $S=I\geq\frac{5}{2}$ are not observed in nature.

Next, we investigate the distribution of shear forces. We recall that for a large nucleus, a situation which is well described in the liquid drop model, the shear forces are given by $s(r)=\gamma\delta(r-R_N)$, where R_N denotes the radius of the nucleus and γ is the surface tension which can be inferred from the Bethe-Weizsäcker formula [22]. A realistic nucleus has no sharp edge, and "finite skin" effects smear out the delta function, but the liquid drop concept and consequences from it remain valid [22,40]. However, a single nucleon is much more diffuse, as can be seen from the LO result in Fig. 1(b) which shows a "very strongly smeared out delta function," and an unambiguous definition of the nucleon radius is not possible (although one may define certain mean square radii; see Sec. V C). The NLO corrections are moderate in the case of the nucleon; see Fig. 1(b). For the Δ, the NLO correction is much more sizable, where we observe that $s(r)$ is clearly depleted and more strongly spread out. Thus, in the rotating soliton picture, the Δ is a larger and an even more diffuse hadron than the nucleon. This is an intuitive and reasonable result. However, for the quantum numbers $S=I\geq\frac{5}{2}$, we find a very different pattern: here, the shear forces develop a node being negative in the inner region and positive in the outer region. A negative distribution of shear forces cannot be associated with a surface tension of a (however diffuse) particle and in fact was not observed in any of the theoretical studies performed so far [9,10,25–31]. The meaning of this result will become clear shortly.

Next, we discuss the pressure. Let us first recall that only the LO result in Fig. 1(c) satisfies the von Laue condition in Eq. (14). This is so because the condition (14) is equivalent to the variational problem of minimizing the soliton mass $\delta M_{\rm sol}=0$ [10]. If we added NLO corrections to $p(r)$ and evaluated them with a soliton profile obtained from the variational problem $\delta M_{\rm rot}=0$, we of course would obtain results satisfying the von Laue condition (14), but at the price of unacceptable violations of chiral symmetry; see the discussion in Sec. V A. If instead we use the LO soliton profile obtained from $\delta M_{\rm sol}=0$, which preserves chiral symmetry, and evaluate $p(r)$ with NLO corrections "added as a small perturbations" as it is customarily done, we obtain the "approximate NLO" results shown in Fig. 1(c). These results do not satisfy the von Laue condition. Interestingly, on the scale of Fig. 1(c), the NLO correction to the nucleon looks moderate, and now we are in the position to quantify this statement. The approximate NLO result for the pressure does not satisfy the von Laue condition (14) exactly, but does so "approximately" since

$$\left[\frac{\int_0^\infty {\rm d}r r^2 p(r)}{\int_0^\infty {\rm d}r r^2|p(r)|}\right]_{\rm NLO,approx,S=\frac{1}{2}}=0.30\sim\mathcal{O}(N_c^{-1}). \quad (31)$$

In this sense the $1/N_c$ corrections in the nucleon case are moderate, and the von Laue condition remains "satisfied" within the accuracy one would expect after adding NLO corrections as a "small perturbation." Another highly sensitive test is provided by evaluating the D-term d_1 from $s(r)$ and $p(r)$ according to Eqs. (15) and (16). In LO, we obtain the consistent result $d^p_{1,\rm LO}=d^s_{1,\rm LO}=-4.48$, where the subscripts indicate whether the value is obtained from $s(r)$ or $p(r)$. If one naively includes NLO corrections, this equivalence is spoiled, and we find $d^p_{1,\rm NLO}=-2.61$ vs $d^s_{1,\rm NLO}=-4.26$. The two results agree within about $24\%\sim\mathcal{O}(N_c^{-1})$, i.e., also within the expected accuracy. It is important to stress that the approximate NLO result for $s(r)$ yields a D term much closer to the LO result than the approximate NLO result for $p(r)$. For Δ and higher-spin states, the NLO corrections to the pressure introduce a major qualitative change: the zero of $p(r)$ disappears,[5] and we find a "100% violation" of the von Laue condition as measured analogous to Eq. (31). However, already the "30% violation" of the von Laue condition for the nucleon in Eq. (31) is not acceptable, as this implies nonconservation of the EMT as explained in Sec. V A.

To obtain an acceptable estimate for the NLO corrections to the pressure and construct a conserved EMT, we have to reconstruct $p(r)$ from $s(r)$ according to Eq. (30). The "reconstructed NLO" results are shown in Fig. 1(d). These results satisfy the von Laue condition (14) which we visualize in Fig. 1(e), which shows the reconstructed NLO results for $r^2p(r)$. We again observe that the effects of NLO corrections for the nucleon are small, and they are more sizable for Δ. However, both states $S=\frac{1}{2},\frac{3}{2}$ exhibit the pattern of a stable physical situation: positive $p(r)$ in the inner region, negative $p(r)$ in the outer region, and exact balance according to the von Laue condition. The situation is fundamentally different for higher-spin states $S\geq\frac{5}{2}$; here, the reconstructed pressure also satisfies the von Laue condition, but the signs are reversed, and there is no balance of forces. The negative $p(r)$ in the center corresponds to attractive forces which are unbalanced; i.e., the inner part of the soliton collapses. At the same time, the positive $p(r)$ in the outer region is also unbalanced, and the repulsive forces expel the outer part of the (too-fast) rotating soliton.

Let us also comment on the local stability criteria. All states satisfy $T_{00}(r)\geq 0$ in agreement with Eq. (17). However, only the states with $S\leq\frac{3}{2}$ comply with the local

[5]Notice that this is for the optimized parameters of Ref. [10]; see Footnote 3. For example, for the parameters of Ref. [33], the NLO effects would be more drastic, and, e.g., the node of $p(r)$ would disappear already for $S=I=\frac{1}{2}$ as shown in Ref. [10].

stability criterion (18), while the states with $S \geq \frac{5}{2}$ violate it as shown in Fig. 1(f). It is important to keep in mind that this is a naive "mechanical picture" which is nevertheless very insightful. The rotating soliton approach predicts all states $S = I = \frac{1}{2}, \frac{3}{2}, \frac{5}{2}, \ldots$ on equal footing. It is therefore remarkable that the approach itself explains that rotating solitons with $S = I \geq \frac{5}{2}$ are artifacts of the rigid rotator quantization as they violate basic mechanical stability criteria and therefore cannot correspond to physical states.

C. Selected results

Having established a consistent scheme to estimate $1/N_c$ corrections to nucleon and Δ properties in the Skyrme model, we end this section by stating some results of interest in the context of EMT densities. For the parameters used in this work, see Footnote 3, we have in LO for the baryon masses $M_\Delta = M_N = 1085$ MeV. Including NLO corrections, we obtain $M_N = 1159$ MeV and $M_\Delta = 1452$ MeV. Thus, the physical values of the masses are described within (20–30)% accuracy, which is typical for this model [39]. Notice that soliton models generally tend to overestimate baryon masses to spurious contributions from rotational and translational zero modes [41].

In Table II, we summarize the Skyrme model predictions for selected EMT properties. Besides the D-term d_1, we include results for the mean square radius of the energy density $\langle r_E^2 \rangle$ and the mean square radius of the shear forces defined as $\langle r_s^2 \rangle = \int_0^\infty \mathrm{d}r r^2 s(r) / \int_0^\infty \mathrm{d}r s(r)$. In addition, we also quote the results for the position R_0 at which the pressure exhibits the node, i.e., $p(R_0) = 0$. The LO results are equal for the nucleon and Δ, but NLO corrections remove this degeneracy. The NLO results for d_1 and R_0 are obtained with the reconstructed NLO result for the pressure.

The results in Table II show that NLO corrections are small for the nucleon and somewhat more sizable for Δ. In both cases, they do not exceed 30%, which one would naturally expect for $1/N_c$ corrections. With NLO corrections included, the D term of the nucleon is -4.48, and that of the Δ is -3.31. Moreover, the Δ is larger than the nucleon, which is quantified by the various radii in Table II. This is an intuitive result and in line with calculations of the electric mean square radius of Δ^+ in models [42] and lattice QCD [43]. The result for the D term of the Δ in Table II is to the best of our knowledge the first calculation of the D term of the Δ resonance. Remarkably, also the D term of the Δ is negative—in agreement with theoretical calculations in other systems [9,10,25–31]; see also Refs. [21,44–51].

TABLE II. Selected EMT properties of the nucleon and Δ from the Skyrme model. The results for the D-term d_1; mean square radii of the energy density and shear forces, $\langle r_E^2 \rangle$ and $\langle r_s^2 \rangle$; and the position R_0 where the pressure distribution exhibits a node refer to LO (where the properties of two baryons are degenerate) and to NLO of the $1/N_c$ expansion.

		NLO	
	LO	Nucleon	Δ resonance
d_1	-4.48	-4.25	-3.31
$\langle r_E^2 \rangle^{1/2}$	0.74 fm	0.75 fm	0.80 fm
$\langle r_s^2 \rangle^{1/2}$	0.63 fm	0.64 fm	0.72 fm
R_0	0.64 fm	0.65 fm	0.83 fm

VI. CHARMONIUM-BARYON BOUND STATES

After the general introduction to the EMT and its practical description in the Skyrme model, we are now in the position to discuss the effective baryon-quarkonium potential.

A. $V_{\rm eff}$ from Skyrme model

Soliton models tend to overestimate baryon masses, and the Skyrme model (with our parameter fixing) is no exception in this respect; see the previous section. To ensure a phenomenologically consistent description, we rescale $V_{\rm eff}$ as

$$V_{\rm eff}(r) = -\alpha \frac{4\pi^2}{b} \left(\frac{g^2}{g_s^2}\right) \frac{M_{\rm physical}}{M_{\rm rot}} [\nu T_{00}(r) - 3p(r)], \quad (32)$$

so the effective potential is correctly normalized with respect to the physical value of the baryon mass in Eq. (23). Notice that one could also refrain from this step and obtain the same results by redefining the value of α. The effective potentials for the nucleon and Δ obtained in this way are shown in Fig. 2. We see that the effects of $1/N_c$ corrections are modest for the nucleon and somewhat more sizable for the Δ resonance. The Skyrme model predictions for $V_{\rm eff}$ shown in Fig. 2 will be used in the following to investigate the dynamics in the nucleon- and Δ-charmonium systems.

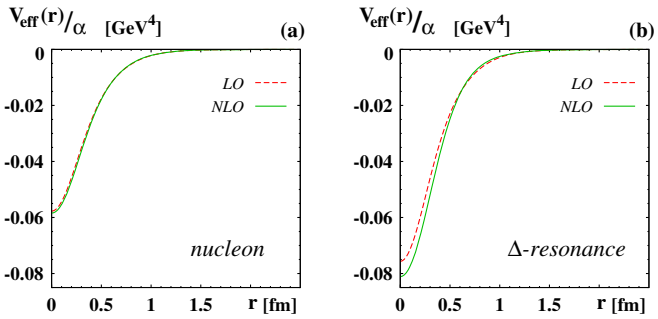

FIG. 2. The effective potential $V_{\rm eff}(r)$ normalized with respect to the polarizability α for (a) the nucleon and (b) Δ as a function of r in LO and NLO order of the large-N_c expansion after the rescaling in Eq. (32); i.e., $V_{\rm eff}(r)$ is normalized according to Eq. (23) with respect to the physical value of the respective baryon mass.

B. Description of quarkonium-baryon bound states

If a baryon-quarkonium bound state exists, its binding energy $E_{\rm bind} < 0$ follows from solving the nonrelativistic Schrödinger equation

$$\left(-\frac{\boldsymbol{\nabla}^2}{2\mu} + V_{\rm eff}(r) - E_{\rm bind}\right)\Psi(\boldsymbol{r}) = 0, \tag{33}$$

where μ is the reduced mass[6] in the channel of interest defined as $\mu^{-1} = M^{-1}_{\rm charmonium} + M^{-1}_{\rm baryon}$.

The Schrödinger equation (33) can be conveniently rewritten using a separation of variables and defining the radial function as follows $\Psi(\boldsymbol{r}) = \Phi_{lm}(\vartheta,\varphi)u_l(r)/r$ with boundary conditions $u_l(r) \propto r^{l+1}$ at small r and $u_{nl}(r) \to 0$ at large r such that it can be normalized as $\int_0^\infty {\rm d}r u_l^2(r) = 1$. In principle, there could be several bound states which should be labeled accordingly by a radial quantum number, but we refrain from this to simplify notation.

Before starting the calculations, let us recall that the shape of $V_{\rm eff}(r)$ and its range, which can be defined, e.g., in terms of $\langle r^2_{\rm eff}\rangle$ in Eq. (24), are determined by the model for the EMT densities and the estimate for the parameter ν in Eq. (4). But the overall normalization of the effective potential is basically unconstrained due to the poor knowledge of the chromoelectric polarizabilities α for which only the rough guidelines in Eq. (2) are available. In practice, it is therefore useful to treat α as a free parameter and vary it in a relatively wide region in order to determine whether bound states exist [8]. Notice that the chromoelectric polarizability of J/ψ in Eq. (2a) is so small and $V_{\rm eff}$ is so shallow that in our formalism no bound states of the nucleon and J/ψ exist—even if we allow the numerical value of $\alpha(1S)$ to vary within a reasonable range. In the following, we will therefore focus on $\Psi(2S)$. Hereby, the lower bound derived in Sec. III will play a very helpful role.

C. Confirmation of $P_c(4450)$ as nucleon-$\psi(2S)$ bound state

The states $P_c(4380)$ and $P_c(4450)$ are observed to decay in the nucleon and J/Ψ; i.e., they have isospin $\frac{1}{2}$ such that it is natural to consider the nucleon channel. However, J/Ψ itself *cannot* form bound states with the nucleon, also because $M_N + M_{J/\Psi} = 4035$ MeV is *smaller* than the mass of the lighter pentaquark $P_c(4380)$. Let us therefore focus here on nucleon-$\psi(2S)$ bound states. In the following, we will quote the numerical results obtained from the Skyrme model in LO and NLO of the $1/N_c$ expansion and confront them with the results from the chiral quark-soliton model (χQSM) reported in Ref. [8] which also refer to LO of the large-N_c limit.

In the eigenvalue problem Eq. (33), threshold bound states (i.e., states with infinitesimally small binding energies) emerge only if the chromoelectric polarizability is above a certain minimal value $\alpha_{\rm min}$ which depends on the orbital angular momentum quantum number l. We obtain for the reduced mass of the nucleon-$\Psi(2S)$ system (the numbers differ only slightly in the nucleon-J/Ψ system)

$$l = 0\colon\ \alpha > \alpha_{\rm min} = \begin{cases} 5.1\ {\rm GeV}^{-3} & {\rm Skyrme,\ LO,} \\ 5.0\ {\rm GeV}^{-3} & {\rm Skyrme,\ NLO,} \\ 5.6\ {\rm GeV}^{-3} & \chi{\rm QSM, Ref.\ [8],} \end{cases} \tag{34}$$

$$l = 1\colon\ \alpha > \alpha_{\rm min} = \begin{cases} 23.8\ {\rm GeV}^{-3} & {\rm Skyrme,\ LO,} \\ 23.5\ {\rm GeV}^{-3} & {\rm Skyrme,\ NLO,} \\ 22.4\ {\rm GeV}^{-3} & \chi{\rm QSM, Ref.\ [8],} \end{cases} \tag{35}$$

Bound states in the channels $l \geq 2$ would require polarizabilities $\alpha > \alpha_{\rm min} = \mathcal{O}(50\text{–}60)\,{\rm GeV}^{-3}$ and higher. A comparison with the guideline (2) for $\alpha(1S)$ reveals that, even if it were energetically possible, J/Ψ could not form bound states with the nucleon. However, for $\psi(2S), \psi(3S), \ldots$, the minimal value of α in the $l = 0$ channel is well below the perturbative guidelines in Eq. (2), which means that the excited charmonia can form s-wave bound states with the nucleon. In the following, we will focus on $\psi(2S)$, leaving the consideration of higher excited charmonia to future work. Notice that the result (34) is in agreement with the bound derived in Sec. III.

Following the procedure of Ref. [8], we now determine which values of $\alpha(2S)$ would be required in order to reproduce in the Skyrme model the exact binding energies $E_{\rm bind} = -176$ MeV of $P_c^+(4450)$ and $E_{\rm bind} = -246$ MeV of $P_c^+(4380)$. The binding energy of the heavier pentaquark state is exactly reproduced for

$$P_c^+(4450)\colon\ \alpha(2S) = \begin{cases} 16.8\ {\rm GeV}^{-3} & {\rm Skyrme,\ LO,} \\ 16.4\ {\rm GeV}^{-3} & {\rm Skyrme,\ NLO,} \\ 17.2\ {\rm GeV}^{-3} & \chi{\rm QSM, Ref.\ [8].} \end{cases} \tag{36}$$

The binding energy of $P_c^+(4380)$ would be exactly reproduced for $\alpha(2S) = (19.6; 19.1; 20.2)\ {\rm GeV}^{-3}$ in the frameworks (Skyrme, LO; Skyrme, NLO; χQSM, Ref. [8]) respectively. These values for α are in reasonable agreement with the perturbative estimate in Eq. (2), but in each

[6] In the recent lattice QCD simulation [52] it was investigated how the potential between a(n) (infinitely heavy) $q\bar{q}$ pair is modified if the heavy $q\bar{q}$ pair is placed inside a light hadron. It was observed that the static potential and consequently also quarkonium masses are reduced by a few MeV. This "medium effect" is analogous to the modification of, e.g., ρ-meson properties in nuclear environment and should not be confused with the binding energy of a heavy $q\bar{q}$ pair with a light hadron, which is described by the effective interaction (1). The results of Ref. [52] imply that in our calculations we should use reduced charmonium masses instead of the physical ones. As other theoretical uncertainties in our approach are more pronounced (heavy-quark mass corrections and $1/N_c$ corrections), we will neglect this small effect.

case, there is only a single bound state. Therefore, we have to choose which of the two pentaquark states can be described in our formalism. The correct identification can be made by considering the decay width.

The decay of a $\Psi(2S)$-nucleon bound state is driven by the potential of the $2S \to 1S$ transition, which has the same "universal shape" as the $V_{\rm eff}$ responsible for the nucleon-$\psi(2S)$ binding mechanism but a significantly smaller normalization due to the small polarizability relevant for the $2S \to 1S$ transition in Eq. (2). As this transition potential is relatively weak, one can use perturbation theory to estimate the decay width as follows [8]:

$$\Gamma = (4\mu q)\left|\int_0^\infty dr r^2 u_l(r) V(r) j_l(qr)\right|^2. \tag{37}$$

Here, q is the center-of-mass momentum $q = \sqrt{2\mu E_R}$, where E_R is the resonance energy, μ is the reduced mass of the decay products, $j_l(z)$ is the spherical Bessel function, and $V_{\rm eff}(r)$ is the potential (22) with the transitional polarizability $|\alpha(2S \to 1S)| = 2\ {\rm GeV}^{-3}$ from phenomenological studies of $\psi' \to J/\psi\pi\pi$ data [13]. For the heavier pentaquark state, we obtain in this way

$$P_c^+(4450){:}\ \Gamma = \begin{cases} 17.0\ {\rm MeV} & {\rm Skyrme,\ LO,} \\ 15.1\ {\rm MeV} & {\rm Skyrme,\ NLO,} \\ 11.2\ {\rm MeV} & \chi{\rm QSM, Ref.\ [8],} \end{cases} \tag{38}$$

which is in reasonable agreement with the observed width of $P_c^+(4450)$ quoted in Table I. For $P_c^+(4380)$, our formalism would yield a similarly narrow width $\Gamma = (21.3; 18.8)\,{\rm GeV}^{-3}$ for (Skyrme, LO; Skyrme, NLO), but the experimental result is an order of magnitude larger; see Table I. Thus, the s-wave nucleon-$\psi(2S)$ bound state found in our approach is clearly identified with the heavier and narrower state $P_c^+(4450)$. The lighter but broader resonance $P_c(4380)$ does not appear to be a nucleon-$\psi(2S)$ bound state.

Our results confirm the interpretation of $P_c^+(4450)$ as a nucleon-$\Psi(2S)$ state [8]. A remarkably consistent and robust picture emerges from our calculation and the comparison to the results of Ref. [8]. For a rather well-constraint value of the chromoelectric polarizability of

$$\alpha(2S) = (16\text{–}17)\ {\rm GeV}^{-3}, \tag{39}$$

two different models of the nucleon, the χQSM used in Ref. [8] and the Skyrme model used in this work, predict a naturally narrow bound state in the $l = 0$ channel of the effective potential (1) which can be identified with $P_c^+(4450)$. The results based on the χQSM in Eqs. (34) and (38) refer to the LO of the $1/N_c$ expansion and are systematically closer to the LO results in the Skyrme model. Comparing the numbers from LO and NLO within the Skyrme model shows that the predictions are also robust with respect to $1/N_c$ corrections.

The approach predicts the following quantum numbers for $P_c^+(4450)$. The vector-meson $\psi(2S)$ has $J^P = 1^-$, and the nucleon has $J^P = \frac{1}{2}^+$. Considering that it is a bound state in the $l = 0$ channel, the parity of $P_c^+(4450)$ is predicted to be negative. The approach predicts actually not one but two states with spins $\frac{1}{2}$ and $\frac{3}{2}$ with a mass difference, caused by hyperfine splitting due to quarkonium-nucleon spin-spin interaction, which is suppressed in the heavy-quark mass limit [8]. The quantum numbers $J^P = \frac{3}{2}^-$ are consistent with experiment; see Table I.

A comment regarding the spin-parity assignment for $P_c^+(4450)$ is in order. The result preferred by the LHCb analysis is $\frac{5}{2}^+$ [1]. The assignments $\frac{5}{2}^-$ and $\frac{3}{2}^-$ are within, respectively, 1 sigma and 2.3 sigma of the preferred fit, i.e., also compatible with data, while assignments like $\frac{1}{2}^\pm$ or $\frac{7}{2}^\pm$ are disfavored at 5-sigma level [1]. Of course, one should keep in mind that the LHCb analysis did not test the hypothesis that the structure around 4450 GeV could consist of two nearly degenerate states with $J^P = \frac{3}{2}^-$ and $J^P = \frac{1}{2}^-$ as predicted in the current approach. It would be very interesting to perform such a test.

D. Prediction of a charmonium-Δ bound state

In Ref. [8], it was argued that not only the nucleon but also other baryons could potentially form bound states with charmonia via the effective interaction (1). With the results obtained on the EMT of Δ in Sec. V, we are in the position to investigate the question of whether Δ can form bound states with charmonia. We will denote the possible charmonium-Δ bound states as $P_{\Delta c}$.

For the effective charmonium-Δ potential $V_{\rm eff}$ to be strong enough to form bound states in the channels with angular momentum l, the polarizabilities must be above the following minimal values:

$$l = 0{:}\ \alpha > \alpha_{\rm min} = \begin{cases} 3.1\ {\rm GeV}^{-3} & {\rm Skyrme,\ LO,} \\ 3.0\ {\rm GeV}^{-3} & {\rm Skyrme,\ NLO,} \end{cases} \tag{40}$$

$$l = 1{:}\ \alpha > \alpha_{\rm min} = \begin{cases} 14.7\ {\rm GeV}^{-3} & {\rm Skyrme,\ LO,} \\ 14.0\ {\rm GeV}^{-3} & {\rm Skyrme,\ NLO,} \end{cases} \tag{41}$$

$$l = 2{:}\ \alpha > \alpha_{\rm min} = \begin{cases} 33.6\ {\rm GeV}^{-3} & {\rm Skyrme,\ LO,} \\ 31.9\ {\rm GeV}^{-3} & {\rm Skyrme, NLO.} \end{cases} \tag{42}$$

Confronting these results with the guideline (2) for $\alpha(1S)$ reveals that J/Ψ cannot bind with Δ. However, $\psi(2S)$ could form bound states with Δ in the $l = 0$ and $l = 1$ channels if we rely on our own estimate (39). This is supported by the model-independent bound in Sec. III.

To proceed with the calculation of possible bound states of Δ and $\psi(2S)$, we will fix $\alpha(2S)$ at the values in Eq. (36) which were required to explain $P_c(4450)$ as a nucleon-$\psi(2S)$ bound state and use the respective LO and NLO

predictions from the Skyrme model for the effective potential as shown in Fig. 2. In this way, we obtain the prediction that there is a single bound state in the $l = 0$ channel with the binding energy and mass

$$l = 0\colon\ E_{\rm bind} = \begin{cases} -370\ {\rm MeV} & {\rm Skyrme,\ LO,} \\ -430\ {\rm MeV} & {\rm Skyrme,\ NLO,} \end{cases}$$
$$\Leftrightarrow M = \begin{cases} 4.54\ {\rm GeV} & {\rm Skyrme,\ LO,} \\ 4.49\ {\rm GeV} & {\rm Skyrme, NLO.} \end{cases} \quad (43)$$

Estimating the width of the new state according to Eq. (37), we obtain

$$l = 0\colon\ \Gamma = \begin{cases} 55\ {\rm MeV} & {\rm Skyrme,\ LO,} \\ 68\ {\rm MeV} & {\rm Skyrme, NLO.} \end{cases} \quad (44)$$

We again observe that the predictions are numerically very stable with respect to model details like effects of $1/N_c$ corrections. The parity of this new state is negative, and the isospin is $\frac{3}{2}$. By applying the arguments of Ref. [8] regarding the spin assignment, we predict that there are three states with $J = \frac{1}{2}, \frac{3}{2}, \frac{5}{2}$ which are mass degenerate modulo heavy-quark mass corrections. In the following, we will refer to this new state as $P_{\Delta c}(4500)$.

Let us now turn to the $l = 1$ channel. In this case, our estimated result for $\alpha(2S)$ in Eq. (39) is much closer to the minimal value of α in Eq. (41), but it is clearly above it, and a single bound state exists although it is loosely bound. The calculation yields

$$l = 1\colon\ E_{\rm bind} = \begin{cases} -25\ {\rm MeV} & {\rm Skyrme,\ LO,} \\ -36\ {\rm MeV} & {\rm Skyrme,\ NLO,} \end{cases}$$
$$\Leftrightarrow M = \begin{cases} 4.89\ {\rm GeV} & {\rm Skyrme,\ LO,} \\ 4.88\ {\rm GeV} & {\rm Skyrme, NLO.} \end{cases} \quad (45)$$

The estimate of the width of the new state according to Eq. (37) yields $\Gamma_2 = (5.0; 9.5)\ {\rm GeV}^{-3}$ for (Skyrme, LO; Skyrme, NLO), but this is not the total width. This state is below the threshold for $\Psi(2S)$-Δ production, but it is above the threshold for $\Psi(2S)$-nucleon-pion production. This means that the Δ in this bound state has the phase space to decay to the pion-nucleon final state without "waiting" for the transition of $\Psi(2S)$ to J/Ψ to occur. The dominant decay mode for this resonance is therefore $P_{\Delta c}(4900) \to \Psi(2S)N\pi$ with a partial decay width $\Gamma_1 \sim 150\ {\rm MeV} \gg \Gamma_2$ which is determined by the width of the Δ. For the total decay width, we therefore predict

$$l = 1\colon\ \Gamma = \Gamma_1 + \Gamma_2 \gtrsim 150\ {\rm MeV} \quad {\rm Skyrme,\ LO\ \&\ NLO.} \quad (46)$$

The parity of this p-wave state is positive, and the isospin is $\frac{3}{2}$. The possible spins are in the range $\frac{1}{2} \le J \le \frac{7}{2}$ following from combining spin 1 of $\Psi(2S)$, spin $\frac{3}{2}$ of Δ, and orbital angular momentum $l = 1$. The different spin states again are mass degenerate in the heavy-quark mass approximation [8]. In practice, heavy-quark mass corrections [8] could shift the masses of (some of) these states into the $\Psi(2S)$-Δ continuum; i.e., they could be presumably even broader. Because of the proximity to the $\Psi(2S)$-Δ threshold, the theoretical uncertainties of this predictions could be larger than in the $l = 0$ channel.

The general reason why a prospective $l = 1$ state appears in the $\Psi(2S)$-Δ system, but not in the $\Psi(2S)$-nucleon system, is related to the larger mass of the Δ which enters the normalization of the potential in Eq. (23). For heavier baryons, lower values for $\alpha_{\rm min}$ are required to form bound states; see Eqs. (34) and (35) vs (40) and (41). This is supported by the model-independent bounds of Sec. III. As a consequence, heavier baryons in general form more easily bound states with charmonia, perhaps even with bottonia.

VII. POSSIBLE WAYS TO OBSERVE $P_{\Delta c}$

In this section, we will discuss possible ways to observe the newly predicted charmonium-Δ bound states $P_{\Delta c}$.

A. $P_{\Delta c}$ and its $SU(3)$ partners in decays of bottom baryons

The pentaquarks P_c were observed in the decay $\Lambda_b^0 \to J/\Psi p K^-$ [1], and their existence is supported by studies of the decay $\Lambda_b^0 \to J/\Psi p \pi^-$ [3]. These weak decays correspond to $b \to c\bar{c}s$ and $b \to c\bar{c}d$ transitions respectively. The second transition is Cabbibo suppressed. In the following, we will discuss both types of transitions.

1. Transitions with $\Delta S = -1$ and $\Delta I = 0$

In this case, the decay $\Lambda_b^0 \to \Delta_c^+ K^- \to J/\Psi p \pi^0 K^-$ is forbidden, and hence the $J/\Psi N\pi\bar{K}$ final state in the decay of Λ_b^0 is not suitable for the search of $P_{\Delta c}$. However, if one considers the final state $J/\Psi N\pi\bar{K}$ in decays of the isospin-1 baryons Σ_b, the isospin-3/2 pentaquarks $P_{\Delta c}$ can be found there. Presumably the most easily detectable modes (no neutral particles in the final state) are

$$\Sigma_b^- \to P_{\Delta c}^0 K^- \to J/\Psi p \pi^- K^-, \quad (47)$$

$$\Sigma_b^+ \to P_{\Delta c}^{++} K^- \to J/\Psi p \pi^+ K^-. \quad (48)$$

We note that $\Delta S = -1$ decays of $\Xi_b \to J/\Psi Y \bar{K}$ (where Y is a baryon with $S = -1$ from the octet or decuplet) are suitable for search of strange flavor $SU(3)$ partners[7] of P_c and $P_{\Delta c}$ pentaquarks. A very interesting possibility to search for $P_{\Omega c}$ (the $S = -3$ decuplet partner of the

[7]On general grounds we expect that $\Psi(2S)$ is more strongly bound to strange members of the octet and decuplet than to nucleon and Δ.

pentaquark $P_{\Delta c}$) is provided by studies of the decay $\Xi_b^0 \to J/\Psi\Omega^- K^+$.

2. Transitions with $\Delta S = 0$ and $\Delta I = \frac{1}{2}$

For such a Cabbibo-suppressed transition, $P_{\Delta c}$ can be searched in Λ_b^0 decays with the final state $J/\Psi N\pi M$ (where M is a isospin-1 meson, e.g., π meson). In decays of Σ_b with the same final state, $P_{\Delta c}$ shows up also for the case where M is an isospin-0 meson, e.g., η meson. In decays of Ξ_b, the pentaquarks $P_{\Delta c}$ can be searched in the final state $J/\Psi N\pi\bar{K}$. Note that the strange octet and decuplet partners of P_c and $P_{\Delta c}$ can be looked for in the same decay mode.

B. $P_{\Delta c}$ formation in photon and meson scattering on the nucleon

In Refs. [53–55], it was suggested to search for P_c pentaquarks through its formation in the process $\gamma + p \to P_c \to J/\Psi + p$. One might think that the search for $P_{\Delta c}$ could be possible in the formation experiment like $\gamma + p \to P_{\Delta c} \to J/\Psi + N + \pi$. However, here we expect that the $\gamma N P_{\Delta c}$ vertex is much smaller than the analogous $\gamma N P_c$ vertex because the former involves isospin-$1/2 \to 3/2$ transition and hence the overwhelming (see the discussion in Ref. [54]) vector dominance $\gamma \to J/\Psi$ transition does not contribute. It seems that the more favorable $P_{\Delta c}$ formation process is

$$\gamma + p \to P_{\Delta c} + \pi \to J/\Psi + N + \pi + \pi. \qquad (49)$$

In such a process, the $\gamma \to J/\Psi$ transition makes a large contribution. The minimal photon energy in a fixed target experiment needed to produce $P_{\Delta c}(4500)$ is 11 GeV, i.e., above the energies accessible in the Gluex Experiment at Jefferson Lab.

In Ref. [56], the formation of P_c pentaquarks was considered in pion-induced processes $\pi + N \to P_c \to J/\Psi + N$. It was shown that the signal cross section is of order 1 nb. Obviously, the $P_{\Delta c}$ pentaquark formation in $\pi + N \to P_{\Delta c} \to J/\Psi + N + \pi$ is of similar size, but probably with smaller background. These reactions could be studied in the charm spectroscopy program at J-PARC, where pion beams with energies up to 20 GeV are available [57].

VIII. CONCLUSIONS

In this work, we made use the formalism of Ref. [8] where the narrow $P_c^+(4450)$ state was interpreted as a nucleon-$\psi(2S)$ s-wave bound state with $J^P = \frac{3}{2}^-$. In the framework of this formalism, we derived a general lower bound which the charmonia chromoelectric polarizabilities must satisfy such that charmonium-baryon bound states can exist and showed in a model-independent way that $\psi(2S)$ can form s-wave bound states with a nucleon and Δ.

Using the Skyrme model for the densities of the EMT, we have confirmed in detail the calculations from Ref. [8] which were based on a different model of the nucleon (chiral quark soliton model). The emerging picture for $P_c^+(4450)$ as a nucleon-$\psi(2S)$ bound state is very robust and insensitive to details of the underlying models. A particulary important aspect of model dependence is related to $1/N_c$ corrections. We have shown that the conclusions and numerical details of the calculations regarding $P_c^+(4450)$ are unaffected by $1/N_c$ corrections.

As an interesting byproduct of our study, we have shown how to construct a conserved EMT when a theory or model cannot be solved exactly and, e.g., $1/N_c$ corrections must be included as a small perturbation. The soliton approach describes baryons with spin and isospin quantum numbers $S = I = \frac{1}{2}, \frac{3}{2}, \frac{5}{2}, \ldots$ in the large-N_c limit. We have shown that, when $1/N_c$ corrections are included, it is possible to construct a conserved EMT with densities which obey fundamental stability criteria only for $S = I = \frac{1}{2}, \frac{3}{2}$ which correspond to a nucleon and Δ. But for $S = I \geq \frac{5}{2}$, the $1/N_c$ corrections are too destabilizing, explaining why such states are not observed in nature.

We have investigated whether charmonia can bind with Δ to produce results which could allow us to further test this approach. We have shown that the approach predicts a negative-parity s-wave bound state in the Δ-$\psi(2S)$ channel with a mass around 4.5 GeV and width around 70 MeV. It also predicts a broader positive-parity p-wave resonance around 4.9 GeV with width of the order of 150 MeV. Each of these states contains several spin states with mass differences (caused by hyperfine splitting due to quarkonium-baryon spin-spin interaction) which are suppressed in the heavy quark mass limit.

An important question concerns how to observe these new pentaquark states. We have examined suitable weak decays of bottom-baryons Λ_b^0, Σ_b, Ξ_b where the new pentaquark states $P_{\Delta c}$ could be observed. We have also discussed how the $P_{\Delta c}$ could be observed in photon-nucleon or pion-nucleon scattering reactions.

An important future direction is to extend the formalism to include charmonium-hyperon bound states. As hyperons are heavier, the formation of such bound states is more favorable to the nucleon case. Particularly interesting new pentaquark states would include charmonium-Ω bound states $P_{\Omega c}$, which include the $S = -3$ decuplet partner of $P_{\Delta c}$, have the minimal content $sssc\bar{c}$, and could be detected in weak decays of $\Xi_b^0 \to J/\Psi\Omega^- K^+$. The properties of these and other hyperon-charmonium bound states will be addressed in future work. As they scale with the size of the system, the chromoelectric polarizabilities of bottonia are too small, and the resulting effective interactions are too weak to form nucleon-bottomium bound states. An interesting open question concerns the possibility of whether the heavier hyperons may form bound states with bottonia. This is another interesting topic to explore in future studies.

ACKNOWLEDGMENTS

This work was initiated by Prof. A. N. Vall to whom we are very indebted and we devote this paper to his memory. M. V. P. is grateful to M. Eides, Yu. Panteleeva and V. Petrov for many illuminating discussions. We also thank Kirill M. Semenov-Tian-Shansky for bringing Ref. [20] to our attention. This work was supported in part by the National Science Foundation (Contract No. 1406298), and the Deutsche Forschungsgemeinschaft (Grant No. VO 1049/1).

APPENDIX: CHIRAL PROPERTIES OF EMT DENSITIES

In this Appendix, we review the large-r behavior of the EMT densities $T_{00}(r), s(r), p(r)$ derived from soliton models in the large-N_c limit. The chiral soliton fields are described in terms of profiles $P(r)$ [9,10]. Although the dynamics of the different models is much different, chiral symmetry uniquely dictates that the profiles exhibit at asymptotic distances, in practice at $r \gtrsim (1\text{–}2)$ fm, the behavior

$$P(r) = \frac{2R_0^2}{r^2}(1 + m_\pi r)\exp(-m_\pi r) + \ldots, \tag{A1}$$

where the dots indicate subleading terms. This behavior is universal, i.e., valid for all (light) baryons in the large-N_c limit. The "soliton size" R_0 is a characteristic and in general model-dependent length scale in the respective model. In the chiral limit, however, it can be related model independently to the axial-coupling constant of the nucleon and the pion decay constant; see Eq. (21).

In the χQSM and the Skyrme model, the large-r behavior of the EMT densities can be computed analytically [9,10]. Retaining only the leading chiral contributions, one obtains from Eq. (A1) the results [10]

$$T_{00}(r) = \frac{1}{2}\frac{F_\pi^2 R_0^4}{r^6}(6 + 12m_\pi r + 11m_\pi^2 r^2 + 6m_\pi^3 r^3 + 2m_\pi^4 r^4)e^{-m_\pi r} + \ldots, \tag{A2a}$$

$$p(r) = -\frac{1}{6}\frac{F_\pi^2 R_0^4}{r^6}(6 + 12m_\pi r + 13m_\pi^2 r^2 + 10m_\pi^3 r^3 + 4m_\pi^4 r^4)e^{-m_\pi r} + \ldots, \tag{A2b}$$

$$s(r) = \frac{1}{2}\frac{F_\pi^2 R_0^4}{r^6}(6 + 12m_\pi r + 14m_\pi^2 r^2 + 8m_\pi^3 r^3 + 2m_\pi^4 r^4)e^{-m_\pi r} + \ldots. \tag{A2c}$$

In the chiral limit, one finds the behavior quoted in Eqs. (20a)–(20b) in the main text, and for $m_\pi \neq 0$, one obtains large-distance behavior

$$T_{00}(r) = F_\pi^2 R_0^4 \frac{m_\pi^4}{r^2} e^{-m_\pi r} + \ldots, \tag{A3a}$$

$$p(r) = -\frac{2}{3} F_\pi^2 R_0^4 \frac{m_\pi^4}{r^2} e^{-m_\pi r} + \ldots, \tag{A3b}$$

$$s(r) = F_\pi^2 R_0^4 \frac{m_\pi^4}{r^2} e^{-m_\pi r} + \ldots \tag{A3c}$$

Notice that Eq. (21) is valid only in the chiral limit. For physical pion masses, Eq. (21) approximates the respective model prediction for g_A within 5% [10].

Although derived in soliton models, these results are practically model independent. In particular, it was shown that they imply the correct chiral behavior of the EMT form factors which coincides with chiral perturbation theory [58,59] if one considers that the large-N_c limit and chiral limit do not commute [9]. The noncommutativity of these limits is caused by the special role of the Δ resonance. In the large-N_c limit, the Δ-nucleon mass splitting vanishes,

$$M_\Delta - M_N \sim \mathcal{O}(N_c^{-1}), \tag{A4}$$

such that chiral loops with the Δ resonance as an intermediate state contribute on the same footing as nucleon intermediate states to chiral properties. The contribution of the Δ to scalar-isoscalar quantities in the large-N_c limit is exactly two times larger than that of the nucleon [60]. Therefore, e.g., the leading nonanalytic contributions to the D term derived from soliton models are three times larger than in chiral perturbation theory [9]. We have taken this into account in Sec. III in our estimates of the Calogero bounds for α by reducing the coefficient in the large-r asymptotics of $V_{\rm eff}(r)$ by factor 3. This resulting bound is a lower and more realistic bound for $N_c = 3$ colors.

It is interesting to inspect the local criterion (18) at asymptotic distances. In the chiral limit, the compliance of with (18) is evident. But for finite m_π, the leading terms from (A2), i.e., the terms displayed in Eq. (A3a) in the main text, cancel out exactly, and the criterion (18) is fulfilled by the subleading chiral terms. The results for both cases are

$$\frac{2}{3}s(r) + p(r) = F_\pi^2 R_0^4 \times \begin{cases} \frac{1}{r^6} & \text{for } m_\pi = 0, \\ \frac{m_\pi^3}{r^3} e^{-m_\pi r} & \text{for } m_\pi \neq 0. \end{cases} \tag{A5}$$

[1] R. Aaij *et al.* (LHCb Collaboration), Phys. Rev. Lett. **115**, 072001 (2015).
[2] R. Aaij *et al.* (LHCb Collaboration), Phys. Rev. Lett. **117**, 082002 (2016).
[3] R. Aaij *et al.* (LHCb Collaboration), Phys. Rev. Lett. **117**, 082003 (2016).
[4] R. Chen, X. Liu, X. Q. Li, and S. L. Zhu, Phys. Rev. Lett. **115**, 132002 (2015); H. X. Chen, W. Chen, X. Liu, T. G. Steele, and S. L. Zhu, Phys. Rev. Lett. **115**, 172001 (2015); L. Roca, J. Nieves, and E. Oset, Phys. Rev. D **92**, 094003 (2015); J. He, Phys. Lett. B **753**, 547 (2016).
[5] L. Maiani, A. D. Polosa, and V. Riquer, Phys. Lett. B **749**, 289 (2015); V. V. Anisovich, M. A. Matveev, J. Nyiri, A. V. Sarantsev, and A. N. Semenova, arXiv:1507.07652; R. F. Lebed, Phys. Lett. B **749**, 454 (2015); G. N. Li, M. He, and X. G. He, J. High Energy Phys. 12 (2015) 128.
[6] A. Mironov and A. Morozov, JETP Lett. **102**, 271 (2015).
[7] U. G. Meißner and J. A. Oller, Phys. Lett. B **751**, 59 (2015); M. Mikhasenko, arXiv:1507.06552; F. K. Guo, U. G. Meißner, W. Wang, and Z. Yang, Phys. Rev. D **92**, 071502 (2015).
[8] M. I. Eides, V. Y. Petrov, and M. V. Polyakov, Phys. Rev. D **93**, 054039 (2016).
[9] K. Goeke, J. Grabis, J. Ossmann, M. V. Polyakov, P. Schweitzer, A. Silva, and D. Urbano, Phys. Rev. D **75**, 094021 (2007).
[10] C. Cebulla, K. Goeke, J. Ossmann, and P. Schweitzer, Nucl. Phys. **A794**, 87 (2007).
[11] E. Witten, Nucl. Phys. **B160**, 57 (1979); **B223**, 433 (1983).
[12] K. Gottfried, Phys. Rev. Lett. **40**, 598 (1978).
[13] M. B. Voloshin, Prog. Part. Nucl. Phys. **61**, 455 (2008).
[14] M. B. Voloshin, Sov. J. Nucl. Phys. **36**, 143 (1982) [Yad. Fiz. **36**, 247 (1982)].
[15] M. E. Peskin, Nucl. Phys. **B156**, 365 (1979); G. Bhanot and M. E. Peskin, Nucl. Phys. **B156**, 391 (1979).
[16] N. Brambilla, G. Krein, J. Tarrús Castellà, and A. Vairo, Phys. Rev. D **93**, 054002 (2016).
[17] N. K. Nielsen, Nucl. Phys. **B120**, 212 (1977); J. C. Collins, A. Duncan, and S. D. Joglekar, Phys. Rev. D **16**, 438 (1977).
[18] V. A. Novikov and M. A. Shifman, Z. Phys. C **8**, 43 (1981).
[19] X. D. Ji, Phys. Rev. Lett. **74**, 1071 (1995); Phys. Rev. D **52**, 271 (1995).
[20] F. Calogero, J. Math. Phys. (N.Y.) **6**, 161 (1965).
[21] H. R. Pagels, Phys. Rev. **144**, 1250 (1966).
[22] M. V. Polyakov, Phys. Lett. B **555**, 57 (2003).
[23] M. von Laue, Ann. Phys. (Berlin) **340**, 524 (1911).
[24] M. V. Polyakov and C. Weiss, Phys. Rev. D **60**, 114017 (1999).
[25] K. Goeke, J. Grabis, J. Ossmann, P. Schweitzer A. Silva, and D. Urbano, Phys. Rev. C **75**, 055207 (2007).
[26] H. C. Kim, P. Schweitzer, and U. Yakhshiev, Phys. Lett. B **718**, 625 (2012).
[27] J. H. Jung, U. Yakhshiev, and H. C. Kim, J. Phys. G **41**, 055107 (2014).
[28] J. H. Jung, U. Yakhshiev, H. C. Kim, and P. Schweitzer, Phys. Rev. D **89**, 114021 (2014).
[29] M. Mai and P. Schweitzer, Phys. Rev. D **86**, 076001 (2012).
[30] M. Mai and P. Schweitzer, Phys. Rev. D **86**, 096002 (2012).
[31] M. Cantara, M. Mai, and P. Schweitzer, Nucl. Phys. **A953**, 1 (2016).
[32] T. H. R. Skyrme, Proc. R. Soc. A **260**, 127 (1961).
[33] G. S. Adkins, C. R. Nappi, and E. Witten, Nucl. Phys. **B228**, 552 (1983).
[34] G. S. Adkins and C. R. Nappi, Nucl. Phys. **B233**, 109 (1984).
[35] E. Guadagnini, Nucl. Phys. **B236**, 35 (1984).
[36] G. S. Adkins and C. R. Nappi, Nucl. Phys. **B249**, 507 (1985).
[37] M. Bander and F. Hayot, Phys. Rev. D **30**, 1837 (1984).
[38] E. Braaten and J. P. Ralston, Phys. Rev. D **31**, 598 (1985).
[39] For reviews, see I. Zahed and G. E. Brown, Phys. Rep. **142**, 1 (1986); G. Holzwarth and B. Schwesinger, Rep. Prog. Phys. **49**, 825 (1986); F. Meier and H. Walliser, Phys. Rep. **289**, 383 (1997).
[40] V. Guzey and M. Siddikov, J. Phys. G **32**, 251 (2006).
[41] P. V. Pobylitsa, E. Ruiz Arriola, T. Meissner, F. Grummer, K. Goeke, and W. Broniowski, J. Phys. G **18**, 1455 (1992).
[42] T. Ledwig, A. Silva, and M. Vanderhaeghen, Phys. Rev. D **79**, 094025 (2009).
[43] C. Alexandrou, T. Korzec, G. Koutsou, Th. Leontiou, C. Lorcé, J. W. Negele, V. Pascalutsa, A. Tsapalis, and M. Vanderhaeghen, Phys. Rev. D **79**, 014507 (2009).
[44] J. F. Donoghue and H. Leutwyler, Z. Phys. C **52**, 343 (1991).B. Kubis and U. G. Meissner, Nucl. Phys. **A671**, 332 (2000) [**A692**, 647(E) (2001)].
[45] X. D. Ji, W. Melnitchouk, and X. Song, Phys. Rev. D **56**, 5511 (1997).
[46] V. Y. Petrov, P. V. Pobylitsa, M. V. Polyakov, I. Börnig, K. Goeke, and C. Weiss, Phys. Rev. D **57**, 4325 (1998).
[47] P. Schweitzer, S. Boffi, and M. Radici, Phys. Rev. D **66**, 114004 (2002).
[48] P. Hägler, J. W. Negele, D. B. Renner, W. Schroers, Th. Lippert, and K. Schilling (LHPC Collaboration), Phys. Rev. D **68**, 034505 (2003); **77**, 094502 (2008); M. Göckeler, R. Horsley, D. Pleiter, P. E. L. Rakow, A. Schäfer, G. Schierholz, and W. Schroers (QCDSF Collaboration), Phys. Rev. Lett. **92**, 042002 (2004); J. D. Bratt *et al.*, Phys. Rev. D **82**, 094502 (2010).
[49] I. R. Gabdrakhmanov and O. V. Teryaev, Phys. Lett. B **716**, 417 (2012).
[50] H. D. Son and H. C. Kim, Phys. Rev. D **90**, 111901 (2014).
[51] B. Pasquini, M. V. Polyakov, and M. Vanderhaeghen, Phys. Lett. B **739**, 133 (2014).
[52] M. Alberti, G. S. Bali, S. Collins, F. Knechtli, G. Moir, and W. Söldner, arXiv:1608.06537.
[53] Q. Wang, X. H. Liu, and Q. Zhao, Phys. Rev. D **92**, 034022 (2015).
[54] V. Kubarovsky and M. B. Voloshin, Phys. Rev. D **92**, 031502 (2015).
[55] M. Karliner and J. L. Rosner, Phys. Lett. B **752**, 329 (2016).
[56] S. H. Kim, H. C. Kim, and A. Hosaka, arXiv:1605.02919.
[57] K. Shirotori *et al.*, J. Phys. Soc. Jpn. Conf. Proc. **8**, 022012 (2015).
[58] J. W. Chen and X. D. Ji, Phys. Rev. Lett. **88**, 052003 (2002); A. V. Belitsky and X. D. Ji, Phys. Lett. B **538**, 289 (2002); S.-I. Ando, J.-W. Chen, and C.-W. Kao, Phys. Rev. D **74**, 094013 (2006).
[59] M. Diehl, A. Manashov, and A. Schäfer, Eur. Phys. J. A **29**, 315 (2006); P. Wein, P. C. Bruns, and A. Schäfer, Phys. Rev. D **89**, 116002 (2014).
[60] T. D. Cohen and W. Broniowski, Phys. Lett. B **292**, 5 (1992).